

An effective method for eigen-problem solution of fluid-structure systems

A. Keivani*, V. Lotfi

Faculty of Civil Engineering, Amirkabir University of Technology, Tehran, Iran

Received 28 August 2012; accepted in revised form 19 April 2013

Abstract

Efficient mode shape extraction of fluid-structure systems is of particular interest in engineering. An efficient modified version of unsymmetric Lanczos method is proposed in this paper. The original unsymmetric Lanczos method was applied to general form of unsymmetric matrices, while the proposed method is developed particularly for the fluid-structure matrices. The method provides us with significant capabilities of symmetric matrix storage scheme and application of real variables in calculations. The efficiency of the proposed method has been examined in mode shape extraction of several dam-water systems and is compared with pseudo subspace method which has identical capabilities. The results show significant time efficiency especially for problems with large dimensions.

Keywords: Fluid-structure, Unsymmetric eigen-problem, Unsymmetric Lanczos, Pseudo subspace.

1. Introduction

Investigations on fluid-structure interaction usually lead to differential equations involving complicated boundary conditions. In absence of analytical solutions, finite element method has been extensively used as an alternative solution [1-4]. Furthermore, pressure and displacement degrees of freedom for fluid and structure domains are usually preferred, respectively.

Under these circumstances, modal solution technique relies on extraction of fluid-structure coupled mode shapes. These vectors, usually, provide us with a more comprehensive insight into the structure behavior. Furthermore, in cases where multiple linear analyses are required, direct approaches are not efficient in comparison with modal approaches. On the other hand, considering that fluid-structure dynamic equations of motion are unsymmetrical, conventional methods are not directly applicable for unsymmetrical eigen-problem solution. In practice, only several initial mode shapes are essential for analysis and therefore methods involving simultaneous computation of all mode shapes, such as family of QR-like Methods [5-7] do not apply. It is also quite apparent that selection of an appropriate method for mode shapes calculation, directly affects the efficiency of modal analysis.

*Corresponding author.

Tel: +989153008754

E-mail address: amir.keivani@gmail.com

Despite the existence of methods for eigen-solution of fluid-structure interaction problems [8], these methods are approximate and do not show sufficient efficiency. Additionally, higher numbers of mode shapes are required as a result of replacing actual mode shapes with the approximate ones. Moreover, there are limited numbers of practical solution methods in the related literature for unsymmetrical eigen-problem with large dimensions. The conventional subspace, inverse iteration, Arnoldi and Lancsoz methods compose the main core of the most of them. Some of them use inexact assumptions in their procedure to enhance efficiency [9-13], while others try to extract exact eigen values and vectors of the system [14-17]. Among the methods that are used for the case of fluid-structure, one may refer to Two-sided Lanczos [14] and Pseudo-symmetric subspace [17] approaches. The Two-sided Lanczos was originally developed for extraction of mode shapes regarding general form of unsymmetrical eigen-problem, while the latter is a developed version of subspace iteration method particularly enhanced to take into consideration especial characteristics of fluid-structure systems eigen-problem.

The aim of this study is to modify unsymmetric Lanczos method to enhance its efficiency by considering contributing characteristics of fluid-structure systems. Therefore, mode shapes regarding several dam-reservoir systems are computed by both modified Lanczos and pseudo-symmetric subspace methods, and the results are compared from computational time efficiency point of view.

2. Dynamic interaction equation of motion

Finite element discretization of dynamic equation of motion assuming pressure degrees of freedom for fluid and displacement for structure, results in the following matrix equation [18]:

$$\begin{bmatrix} \mathbf{M} & \mathbf{0} \\ \mathbf{B} & \mathbf{G} \end{bmatrix} \begin{Bmatrix} \dot{\mathbf{r}} \\ \dot{\mathbf{p}} \end{Bmatrix} + \begin{bmatrix} \mathbf{C} & \mathbf{0} \\ \mathbf{0} & \mathbf{L} \end{bmatrix} \begin{Bmatrix} \dot{\mathbf{r}} \\ \dot{\mathbf{p}} \end{Bmatrix} + \begin{bmatrix} \mathbf{K} & -\mathbf{B}^T \\ \mathbf{0} & \mathbf{H} \end{bmatrix} \begin{Bmatrix} \mathbf{r} \\ \mathbf{p} \end{Bmatrix} = \begin{bmatrix} -\mathbf{M}\mathbf{J}\mathbf{a}_g \\ -\mathbf{B}\mathbf{J}\mathbf{a}_g \end{bmatrix} \quad (1)$$

where, \mathbf{K} , \mathbf{M} and \mathbf{C} are stiffness, mass and damping matrices of the solid region and \mathbf{H} , \mathbf{G} , \mathbf{L} are corresponding matrices of the fluid domain. Also, \mathbf{B} is referred to as the interaction matrix, while \mathbf{J} is the influence matrix with its three columns represent rigid body motions in the three directions. Moreover, \mathbf{a}_g is the vector of ground accelerations.

Referring to equation (1), matrix \mathbf{B} has caused un-symmetry in the generalized stiffness and mass matrices. Solution of equation (1), can be carried out in time domain by direct integration methods. However, modal superposition approach is usually preferred as an alternative for their efficiency.

3. Modal analysis

Dynamic equation of motion for a fluid-structure system represented by equation (1), may be written in a compact form as follows:

$$\overline{\mathbf{M}}\ddot{\bar{\mathbf{r}}} + \overline{\mathbf{C}}\dot{\bar{\mathbf{r}}} + \overline{\mathbf{K}}\bar{\mathbf{r}} = -\overline{\mathbf{M}}\overline{\mathbf{J}}\mathbf{a}_g \quad (2)$$

with the following definitions for $\bar{\mathbf{r}}$ and $\overline{\mathbf{J}}$:

$$\bar{\mathbf{r}} = \begin{bmatrix} \mathbf{r} \\ \mathbf{p} \end{bmatrix} \quad (3a)$$

$$\overline{\mathbf{J}} = \begin{bmatrix} \mathbf{J} \\ \mathbf{0} \end{bmatrix} \quad (3b)$$

In applying modal analysis, it is required to extract several mode shapes of the system. Consequently, the following eigen-problem should be solved:

$$\bar{\mathbf{K}} \mathbf{X}_j^R = \lambda_j \bar{\mathbf{M}} \mathbf{X}_j^R \quad (4)$$

In which, generalized stiffness and mass matrices are introduced as:

$$\bar{\mathbf{K}} = \begin{bmatrix} \mathbf{K} & -\mathbf{B}^T \\ \mathbf{0} & \mathbf{H} \end{bmatrix} \quad (5a)$$

$$\bar{\mathbf{M}} = \begin{bmatrix} \mathbf{M} & \mathbf{0} \\ \mathbf{B} & \mathbf{G} \end{bmatrix} \quad (5b)$$

It is noted that generalized stiffness and mass matrices have un-symmetric forms. This will mathematically culminate into two sets of right and left-mode shapes for the eigen-problem. The left-mode shape vectors can be extracted through the following relation:

$$\bar{\mathbf{K}}^T \mathbf{X}_j^L = \lambda_j \bar{\mathbf{M}}^T \mathbf{X}_j^L \quad (6)$$

Herein, \mathbf{X}_j^R and \mathbf{X}_j^L represent j-th right and left-mode shapes of the system, respectively. It is worthwhile to mention that eigenvalues obtained through relations (4) and (6) are essentially the same. This is due to the fact that corresponding determinant expansion of these eigen-problems are equal. However, their eigenvectors are not equal. Therefore, in order to benefit from orthogonality relation, both right and left vectors must be calculated. The efficient extraction process of these eigenvectors will be discussed below in details.

4. Unsymmetrical eigen-problem solution

The key factor in efficiency of modal analysis is to devise an effective and computationally efficient approach for extraction of mode shapes and natural frequencies of the considered system. As previously mentioned, assuming pressure and displacement degrees of freedom will lead to an unsymmetrical generalized mass and stiffness matrices. Conventional procedures for eigen-problem solution are not directly applicable since they are usually developed for symmetric matrices and consequently use the advantage of sparse characteristics of symmetric matrices. Furthermore, general form of unsymmetrical matrices could lead to solutions with complex-number eigenvalues. Thus, general eigen-solvers employ complex-number arithmetic in their solution process. On the other hand, real eigenvalues are physically expected in fluid-structure problems.

One possible solution for eigen-problem especial to fluid-structure interaction was proposed by Iron [19]. His method was based on symmetrization in which considerable amount of mathematical computation was required. Fellipa and coworkers [20] presented a method by including additional potential variables doubling the dimension of original problem. Sandberg [8] proposed a method for approximate mode extraction of the system, where decoupled mode shapes of solid and fluid regions were used to evaluate coupled mode shapes. Two-sided Lanczos method was proposed by Rajakumar & Rojer [14] for general form of unsymmetric matrices with complex variable in the calculation process. This method had taken advantage of solving system of equation to avoid stiffness matrix inversion. Pseudo-symmetric subspace method was developed by Lotfi and Aftabi [17], particularly for the special case of fluid-structure systems. The method included several special purpose matrix operations to comply with interaction problem. Moreover, application of symmetric matrices and real-number arithmetic are among its advantages. In this study, Pseudo-symmetric subspace and Two-sided Lanczos methods will be reviewed briefly, and a proposed method is presented based on modification of Two-sided Lanczos approach. The modified Lanczos method is adopted herein to comply with fluid-structure interaction problem.

4.1. Pseudo-symmetric subspace [17]

In this method, the initial estimate for right modal matrix denoted by \mathbf{X}^R , will be used to approximate vector $\tilde{\mathbf{X}}$ through the following relation:

$$\overline{\mathbf{K}} \tilde{\mathbf{X}} = \overline{\mathbf{M}} \mathbf{X}^R \tag{7}$$

However, to benefit from skyline storage scheme, the following will replace equation (7):

$$\overline{\mathbf{K}}^1 \tilde{\mathbf{X}} = \overline{\mathbf{M}}^2 \mathbf{X}^R \tag{8}$$

In the above relation, operators $(^1, ^2)$ indicate two special purpose operators which are defined in the appendix. Additionally, $\overline{\mathbf{K}}$ and $\overline{\mathbf{M}}$ are symmetric matrices defined as:

$$\overline{\mathbf{K}} = \begin{bmatrix} \mathbf{K} & -\mathbf{B}^T \\ -\mathbf{B} & \mathbf{H} \end{bmatrix} \tag{9a}$$

$$\overline{\mathbf{M}} = \begin{bmatrix} \mathbf{M} & \mathbf{B}^T \\ \mathbf{B} & \mathbf{G} \end{bmatrix} \tag{9b}$$

Applying $\tilde{\mathbf{X}}$ matrix to project $\overline{\mathbf{K}}$ and $\overline{\mathbf{M}}$ matrices leads to an unsymmetrical eigenproblem in the subspace core. To avoid this, $\hat{\mathbf{K}}$ and $\hat{\mathbf{M}}$ are introduced as substitutions with the following definitions:

$$\hat{\mathbf{K}} = \begin{bmatrix} \mathbf{K} & \mathbf{0} \\ \mathbf{0} & \mathbf{G} \end{bmatrix} \tag{10a}$$

$$\hat{\mathbf{M}} = \begin{bmatrix} (\mathbf{M} + \mathbf{B}^T \mathbf{H}^{-1} \mathbf{B}) & \mathbf{B}^T \mathbf{H}^{-1} \mathbf{G} \\ \mathbf{G}^T \mathbf{H}^{-1} \mathbf{B} & \mathbf{G}^T \mathbf{H}^{-1} \mathbf{G} \end{bmatrix} \tag{10b}$$

It can be proved (refer to [17] for details) that eigenvalues and eigenvectors corresponding to these substituted matrices are equal to those given in equation (5). Therefore, these two matrices are used for projection purposes:

$$\mathbf{K}^* = \tilde{\mathbf{X}}^T \hat{\mathbf{K}} \tilde{\mathbf{X}} \tag{11a}$$

$$\mathbf{M}^* = \tilde{\mathbf{X}}^T \hat{\mathbf{M}} \tilde{\mathbf{X}} \tag{11b}$$

where, \mathbf{K}^* and \mathbf{M}^* are projections of $\hat{\mathbf{K}}$ and $\hat{\mathbf{M}}$, respectively. The projected matrices have dimensions which are normally much smaller than those of $\hat{\mathbf{K}}$ or $\hat{\mathbf{M}}$. Moreover, equation (11a) can be simply written in terms of $\tilde{\mathbf{X}}$, $\overline{\mathbf{K}}$ and $\overline{\mathbf{M}}$ as below:

$$\mathbf{K}^* = \tilde{\mathbf{X}}^T (\overline{\mathbf{K}}^3 \tilde{\mathbf{X}} + \overline{\mathbf{M}}^4 \tilde{\mathbf{X}}) \tag{12}$$

In contrast, equation(11-b) can not be directly evaluated due to computational difficulty in term \mathbf{H}^{-1} in $\hat{\mathbf{M}}$ matrix. Thus, a special technique is applied which is summarized below:

Let us partition matrix $\tilde{\mathbf{X}}$ into two parts such that upper and lower parts correspond to solid and fluid degrees of freedom, respectively.

$$\tilde{\mathbf{X}} = \begin{bmatrix} \tilde{\mathbf{X}}_1 \\ \tilde{\mathbf{X}}_2 \end{bmatrix} \tag{13}$$

Moreover, it is easily verifiable that $\hat{\mathbf{M}}$ may be written as:

$$\hat{\mathbf{M}} = \begin{bmatrix} \mathbf{I} & \mathbf{B}^T \\ \mathbf{0} & \mathbf{G} \end{bmatrix} \begin{bmatrix} \mathbf{M} & \mathbf{0} \\ \mathbf{0} & \mathbf{H}^{-1} \end{bmatrix} \begin{bmatrix} \mathbf{I} & \mathbf{0} \\ \mathbf{B} & \mathbf{G} \end{bmatrix} \tag{14}$$

Consequently, by substituting relations (13), (14) into equation (11b), one would have:

$$\mathbf{M}^* = \begin{bmatrix} \tilde{\mathbf{X}}_1^T & \tilde{\mathbf{X}}_2^T \end{bmatrix} \begin{bmatrix} \mathbf{I} & \mathbf{B}^T \\ \mathbf{0} & \mathbf{G} \end{bmatrix} \begin{bmatrix} \mathbf{M} & \mathbf{0} \\ \mathbf{0} & \mathbf{H}^{-1} \end{bmatrix} \begin{bmatrix} \mathbf{I} & \mathbf{0} \\ \mathbf{B} & \mathbf{G} \end{bmatrix} \begin{bmatrix} \tilde{\mathbf{X}}_1 \\ \tilde{\mathbf{X}}_2 \end{bmatrix} \quad (15)$$

Or in more compacted form as:

$$\mathbf{M}^* = \mathbf{Y}^T \mathbf{Z} \quad (16)$$

With the following definitions for \mathbf{Y} and \mathbf{Z} matrices:

$$\mathbf{Y} = \begin{bmatrix} \mathbf{I} & \mathbf{0} \\ \mathbf{B} & \mathbf{G} \end{bmatrix} \begin{bmatrix} \tilde{\mathbf{X}}_1 \\ \tilde{\mathbf{X}}_2 \end{bmatrix} \quad (17)$$

$$\mathbf{Z} = \begin{bmatrix} \mathbf{M} & \mathbf{0} \\ \mathbf{0} & \mathbf{H}^{-1} \end{bmatrix} \mathbf{Y} \quad (18)$$

Applying matrix operator $\overset{6}{*}$, \mathbf{Y} matrix is given as:

$$\mathbf{Y} = \begin{bmatrix} \tilde{\mathbf{X}}_1 \\ \mathbf{0} \end{bmatrix} + \overline{\overline{\mathbf{M}}}^6 \tilde{\mathbf{X}} \quad (19)$$

To obtain \mathbf{Z} vector, the part corresponding to fluid DOFs (i.e., \mathbf{Z}_2) are initially calculated. This is achieved through the following relation with avoiding the inversion of matrix \mathbf{H} which is computationally inefficient.

$$\overline{\overline{\mathbf{K}}}^4 \begin{bmatrix} \mathbf{0} \\ \mathbf{Z}_2 \end{bmatrix} = \begin{bmatrix} \mathbf{0} \\ \mathbf{Y}_2 \end{bmatrix} \quad (20)$$

Thereafter, overall \mathbf{Z} matrix can be written as:

$$\mathbf{Z} = \begin{bmatrix} \mathbf{0} \\ \mathbf{Z}_2 \end{bmatrix} + \overline{\overline{\mathbf{M}}}^3 \tilde{\mathbf{X}}. \quad (21)$$

Obtaining \mathbf{Z} and \mathbf{Y} matrices, \mathbf{M}^* is readily computed. The next step is to find all eigenvalues and eigenvectors of core eigen-problem expressed as:

$$\mathbf{K}^* \mathbf{Q} = \mathbf{M}^* \mathbf{Q} \overline{\overline{\mathbf{\Lambda}}} \quad (22)$$

Herein, the modal matrix is denoted by \mathbf{Q} and the diagonal matrix $\overline{\overline{\mathbf{\Lambda}}}$ consists of eigenvalues. Subsequently, a better estimate for right modal matrix \mathbf{X}^R is obtained through the following relation:

$$\mathbf{X}^R = \tilde{\mathbf{X}} \mathbf{Q} \quad (23)$$

This iterative process continues until convergence. Finally, matrices $\overline{\overline{\mathbf{\Lambda}}}$, \mathbf{X}^R will have the smallest eigenvalues of the original unsymmetric problem (4) and its corresponding right eigenvectors.

The relation between left and right eigenvectors

Although, pseudo-symmetric subspace method leads to right modal matrix, computation of left modal matrix is required to benefit from orthogonal characteristics of mode shapes. In fact, it is proven that there exists a relation between the left and right modal matrices as follows (refer to [17] for details):

$$\begin{bmatrix} \mathbf{X}_1^L \\ \mathbf{X}_2^L \end{bmatrix} = \begin{bmatrix} \mathbf{X}_1^R \\ \mathbf{X}_2^R \overline{\overline{\mathbf{\Lambda}}}^{-1} \end{bmatrix} \quad (24)$$

4.2. Two-sided Lanczos

In order to obtain right and left Lanczos vectors, recursive equations are implemented in two-sided Lanczos method based on two right and left Krylof subspaces. Right and left Krylof subspaces are generated from initial orthogonal vectors \mathbf{V}_1 and \mathbf{W}_1 and may be written as:

$$\mathbf{V}^k = [\mathbf{V}_1 \quad (\bar{\mathbf{K}}^{-1}\bar{\mathbf{M}})\mathbf{V}_1 \quad \dots \quad (\bar{\mathbf{K}}^{-1}\bar{\mathbf{M}})^{m-1}\mathbf{V}_1] \quad (25a)$$

$$\mathbf{W}^k = [\mathbf{W}_1 \quad (\bar{\mathbf{K}}^{-T}\bar{\mathbf{M}}^T)\mathbf{W}_1 \quad \dots \quad (\bar{\mathbf{K}}^{-T}\bar{\mathbf{M}}^T)^{m-1}\mathbf{W}_1] \quad (25b)$$

In fact, these two subspaces are composed of linear combination of right and left eigenvectors of

$$\bar{\mathbf{K}}^{-1}\bar{\mathbf{M}}\mathbf{X}_j^R = \frac{1}{\lambda_j}\mathbf{X}_j^R. \quad (26)$$

This is the same as the eigen-problem of relation (4). Two-sided Lanczos method tries to extract independent eigenvectors from right and left Krylof subspaces. The extracted vectors may be expressed as:

$$\mathbf{V} = [\mathbf{V}_1 \quad \mathbf{V}_2 \quad \dots \quad \mathbf{V}_m] \quad (27a)$$

$$\mathbf{W} = [\mathbf{W}_1 \quad \mathbf{W}_2 \quad \dots \quad \mathbf{W}_m] \quad (27b)$$

The recursive equations which produce Lanczos vectors are presented by the following steps:

1. Initial vectors \mathbf{V}_1 and \mathbf{W}_1 are selected such that it satisfies the following relation:

$$\mathbf{W}_1^T \bar{\mathbf{M}} \mathbf{V}_1 = 1 \quad (28)$$

2. For step j , $\bar{\mathbf{V}}_{j+1}$ and $\bar{\mathbf{W}}_{j+1}$ are computed through equations (29a-b)

$$\bar{\mathbf{V}}_{j+1} = \bar{\mathbf{K}}^{-1}\bar{\mathbf{M}}\mathbf{V}_j - \alpha_j\mathbf{V}_j - \beta_j\mathbf{V}_{j-1} \quad (29a)$$

$$\bar{\mathbf{W}}_{j+1} = \bar{\mathbf{K}}^{-T}\bar{\mathbf{M}}^T\mathbf{W}_j - \alpha_j\mathbf{W}_j - \delta_j\mathbf{W}_{j-1} \quad (29b)$$

where, \mathbf{V}_j , \mathbf{W}_j are the j -th and \mathbf{V}_{j-1} , \mathbf{W}_{j-1} are $(j-1)$ -th right and left vectors. Coefficients α_j , β_j and δ_j are given by:

$$\alpha_j = \mathbf{W}_j^T \bar{\mathbf{M}} \bar{\mathbf{K}}^{-1} \bar{\mathbf{M}} \mathbf{V}_j \quad (30a)$$

$$\delta_{j+1} = \left| \bar{\mathbf{W}}_{j+1}^T \bar{\mathbf{M}} \bar{\mathbf{V}}_{j+1} \right|^{1/2} \quad (30b)$$

$$\beta_{j+1} = \delta_{j+1} \text{Sign}(\bar{\mathbf{W}}_{j+1}^T \bar{\mathbf{M}} \bar{\mathbf{V}}_{j+1}) \quad (30c)$$

In the above equations, $\beta_1\mathbf{V}_0$ and $\delta_1\mathbf{W}_0$ are assumed null vectors in the first step. Additionally, if δ_{j+1} equals to zero, initial vectors (\mathbf{V}_1 and \mathbf{W}_1) should be reselected and the recursive process restarted.

3. Finding β_j and δ_j , the resulting right and left Lanczos vectors are evaluated by

$$\mathbf{V}_{j+1} = \frac{\bar{\mathbf{V}}_{j+1}}{\delta_{j+1}} \quad (31a)$$

$$\mathbf{W}_{j+1} = \frac{\bar{\mathbf{W}}_{j+1}}{\beta_{j+1}} \quad (31b)$$

4. Then, matrix \mathbf{T} is defined by employing coefficients α_j , β_j and δ_j as below:

$$\mathbf{T} = \begin{bmatrix} \alpha_1 & \beta_1 & & & \mathbf{0} \\ \delta_1 & \alpha_2 & & & \\ & & \ddots & & \\ & & & \alpha_{m-1} & \beta_m \\ \mathbf{0} & & & \delta_m & \alpha_m \end{bmatrix} \quad (32)$$

It can be shown that right Lanczos vectors of equation (27a) are related to eigenvectors of \mathbf{T} matrix by the following equation:

$$\mathbf{X}_i^R = \mathbf{V} \bar{\mathbf{Y}}_i \quad (33)$$

where, $\bar{\mathbf{Y}}_i$ results from:

$$\mathbf{T} \bar{\mathbf{Y}}_i = \mu_i \bar{\mathbf{Y}}_i \quad (34)$$

Moreover, μ_i is the i -th eigenvalue of relation (34). Subsequently, eigenvalues of equations (26) and (34) are related as below:

$$\lambda_i = \frac{1}{\mu_i} \quad (35)$$

In the recursive process of Lanczos method, vectors \mathbf{V}_j and \mathbf{W}_j may lose their orthogonality characteristics due to precision error. Therefore, computed vectors should be normalized to the previously calculated vectors. This is achieved through Gram-Schmidt orthogonalization in j -th step. As a result, series of coefficients θ_i and ϕ_i (for $i=1,2,\dots,j$) must be obtained as:

$$\theta_i = \mathbf{W}_i^T \bar{\mathbf{M}} \mathbf{V}_{j+1} \quad (36a)$$

$$\phi_i = \mathbf{V}_i^T \bar{\mathbf{M}}^T \mathbf{W}_{j+1} \quad (36b)$$

If any of θ_i and ϕ_i coefficients surpasses the specified error (ε), the participating fraction of the i th vector should be subtracted from j th vector. This is achieved by the following substitutions:

$$\mathbf{V}_{j+1} \leftarrow \mathbf{V}_{j+1} - \theta_i \mathbf{V}_i \quad (37a)$$

$$\mathbf{W}_{j+1} \leftarrow \mathbf{W}_{j+1} - \phi_i \mathbf{W}_i \quad (37b)$$

4.3. Modified unsymmetric Lanczos method

The two-sided Lanczos method is developed and adopted for fluid-structure interaction in the present study. Furthermore, in order to increase efficiency, generalized mass and stiffness matrices (defined in equations (9a-b)) are stored by skyline storage scheme. Accordingly, particular matrix operations similar to Pseudo-symmetric subspace method are introduced to comply with symmetric matrices. These two operators are presented in appendix and denoted by $\overset{1}{(*)}$ and $\overset{2}{(*)}$. Steps forming modified unsymmetric Lanczos are presented as follows:

1. Initial vectors \mathbf{V}_1 and \mathbf{W}_1 are defined merely by one non-zero element. That is, the first element of \mathbf{V}_1 is assumed to be unity and the first element of \mathbf{W}_1 is defined as the inverse of the first diagonal element of $\bar{\mathbf{M}}$. These assumptions satisfy equation (28). It was observed by experience that these assumptions work effectively and, there was no need to restart the initial vectors.

2. $\tilde{\mathbf{V}}_j$ and $\tilde{\mathbf{W}}_j$ are defined by matrix operations below

$$\tilde{\mathbf{V}}_j = \overline{\overline{\mathbf{M}}}^2 * \mathbf{V}_j \tag{38a}$$

$$\tilde{\mathbf{W}}_j = \overline{\overline{\mathbf{M}}}^1 * \tilde{\mathbf{V}}_j \tag{38b}$$

Applying operators $(*)^1$ and $(*)^2$, the following equations are solved to prevent $\overline{\mathbf{K}}^{-1}$ and $\overline{\mathbf{K}}^{-T}$ calculations:

$$\overline{\overline{\mathbf{K}}}^1 * \overline{\overline{\mathbf{V}}}_j = \tilde{\mathbf{V}}_j \tag{39a}$$

$$\overline{\overline{\mathbf{K}}}^2 * \overline{\overline{\mathbf{W}}}_j = \tilde{\mathbf{W}}_j \tag{39b}$$

Accordingly, equations (29a-b) are written as:

$$\overline{\overline{\mathbf{V}}}_{j+1} = \overline{\overline{\mathbf{V}}}_j - \alpha_j \mathbf{V}_j - \beta_j \mathbf{V}_{j-1} \tag{40a}$$

$$\overline{\overline{\mathbf{W}}}_{j+1} = \overline{\overline{\mathbf{W}}}_j - \alpha_j \mathbf{W}_j - \delta_j \mathbf{W}_{j-1} \tag{40b}$$

where, for $j=1,2,\dots, m$, α_j is given by

$$\alpha_j = \mathbf{W}_j^T (\overline{\overline{\mathbf{M}}}^2 * \overline{\overline{\mathbf{V}}}_j) \tag{41}$$

Likewise, δ_{j+1} and β_{j+1} are obtained by utilizing intermediate variable γ :

$$\gamma = \overline{\overline{\mathbf{W}}}_{j+1}^T (\overline{\overline{\mathbf{M}}}^2 * \overline{\overline{\mathbf{V}}}_{j+1}) \tag{42a}$$

$$\delta_{j+1} = |\gamma|^{1/2} \tag{42b}$$

$$\beta_{j+1} = |\gamma|^{1/2} \text{Sign}(\gamma) \tag{42c}$$

Moreover, right and left vectors are given by

$$\mathbf{V}_{j+1} = \frac{\overline{\overline{\mathbf{V}}}_{j+1}}{\delta_{j+1}} \tag{43a}$$

$$\mathbf{W}_{j+1} = \frac{\overline{\overline{\mathbf{W}}}_{j+1}}{\beta_{j+1}} \tag{43b}$$

3. Orthogonality of the current vectors should be controlled with respect to previously obtained vectors in this step. Coefficients θ_i and ϕ_i represent the numerical error and for $i=1, 2,\dots, j$ are written as:

$$\theta_i = \mathbf{W}_i^T (\overline{\overline{\mathbf{M}}}^1 * \mathbf{V}_{j+1}) \tag{44a}$$

$$\phi_i = \mathbf{V}_i^T (\overline{\overline{\mathbf{M}}}^2 * \mathbf{W}_{j+1}) \tag{44b}$$

If values of θ_i and ϕ_i exceeds the tolerance ε (assumed 10^{-12} herein), \mathbf{V}_j and \mathbf{W}_j are corrected as follows:

$$\mathbf{V}_{j+1} \leftarrow \mathbf{V}_{j+1} - \theta_i \mathbf{V}_i \tag{45a}$$

$$\mathbf{W}_{j+1} \leftarrow \mathbf{W}_{j+1} - \phi_i \mathbf{W}_i \tag{45b}$$

4. Matrix \mathbf{T} is constructed by employing α_j , β_j and δ_j . Eigenvalues and eigenvectors of \mathbf{T} are extracted by QR method, both in [14] and the present study. However, real arithmetic are employed herein, while [14] utilizes complex number arithmetic. As mentioned, eigenvalues and eigen-vectors of \mathbf{T} are referred to as μ_i and $\overline{\mathbf{V}}_i$, respectively.

5. Finally, a more accurate evaluation for eigenvalues of the original eigen-problem is obtained by:

$$\bar{\lambda}_j = \frac{1}{\mu_j}$$

where, $\bar{\lambda}_j$ is a new eigen-value estimate for the original eigen-problem of relation (4). In the present study, a convergence criterion is applied to the relative difference of eigenvalues. Therefore, when m modes shapes are requested for modal analysis, steps 1 to 5 are carried out for $j=1-m$ and eigenvalues are stored. The steps are repeated for $j=m+1$ and calculated eigenvalues are compared to previously stored values. This process continues until convergence is achieved.

6. For converged eigenvalues corresponding to eigenvectors of relation (4), eigenvectors are computed through the following relation:

$$\mathbf{X}_j^R = \mathbf{V} \bar{\mathbf{Y}}_j$$

Likewise, left-eigenvectors \mathbf{X}_j^L are attainable as:

$$\begin{bmatrix} \mathbf{X}_1^L \\ \mathbf{X}_2^L \end{bmatrix} = \begin{bmatrix} \mathbf{X}_1^R \\ \mathbf{X}_2^R \bar{\Lambda}^{-1} \end{bmatrix}.$$

5. Numerical examples

To investigate the efficiency of proposed method, Morrow Point arch dam has been considered as an example. The actual geometry of the dam is not completely symmetrical. However, a symmetric shape is assumed in this study based on average characteristics of the two sides. Details about the geometry can be found elsewhere [21]. Furthermore, to consider the effect of number of degrees of freedom on efficiency, six models of dam-reservoir system are employed with different reservoir's length to height ratio (L/H). The dam body and water domain are discretized by 20-node isoparametric solid and fluid finite elements, respectively (Figure 1). Moreover, dam foundation is assumed to be rigid. Details about finite element meshes are presented in Table 1.

Table 1. Employed finite element meshes of Morrow Point dam-reservoir system

Case	L/H	Number of Fluid Elements	Number of Solid Elements	Number of DOFs	F.E. Nodes
M1	0.2	80	80	1600	867
M2	1	200	80	2035	1416
M3	2	360	80	2615	2148
M4	3	520	80	3195	2880
M5	4	680	80	3775	3612
M6	5	800	80	4210	4161

Material properties of the dam's concrete and water in the reservoir are as follows: for dam concrete: $E=27.6$ GPa, $\nu=0.2$, $\gamma=24.8$ kN/m³ and for water: $\gamma=10$ kN/m³, $c=1440$ m/s

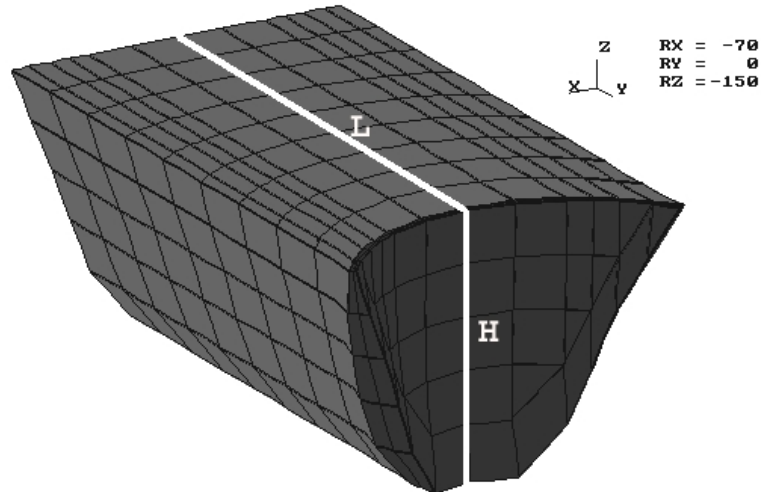


Figure 1. Finite element model of Morrow Point dam-reservoir system (Case M3)

6. Results

First ten natural frequencies corresponding to the six considered cases are presented in Table 2. Results are in perfect agreement up to 6 digits of precision for Pseudo-symmetric subspace and modified Lanczos methods.

Table 2. First ten natural frequencies for different dam-reservoir systems

Mode	Frequency (Hz)					
	M1	M2	M3	M4	M5	M6
1	2.175183	2.672877	2.757409	2.777660	2.782834	2.784269
2	2.729675	2.898059	2.900270	2.901094	2.901540	2.903250
3	3.615446	3.529504	3.329356	3.186721	3.114105	3.078282
4	4.625017	4.715365	3.961621	3.654251	3.503121	3.389050
5	5.176523	5.121203	4.749193	4.411563	3.956438	3.726161
6	5.953851	5.806258	5.378074	4.767045	4.674109	4.243897
7	6.380528	6.448869	5.820010	5.502954	4.813074	4.745078
8	7.598223	6.631286	6.458877	5.822204	5.578247	4.951905
9	8.101044	7.596188	6.464148	6.361083	5.823358	5.630349
10	8.409273	7.768780	7.321584	6.462707	6.291406	5.827240

Figures 2-5 demonstrate the first two right and left-mode shapes of dam-reservoir system for the case M3. It is observed that left and right dam mode shapes have identical displacement values (dam domain). However, pressure distribution (water domain) differs on contour values, while contour shapes remain the same. This verifies the relation between right and left-mode shapes given in equation (24).

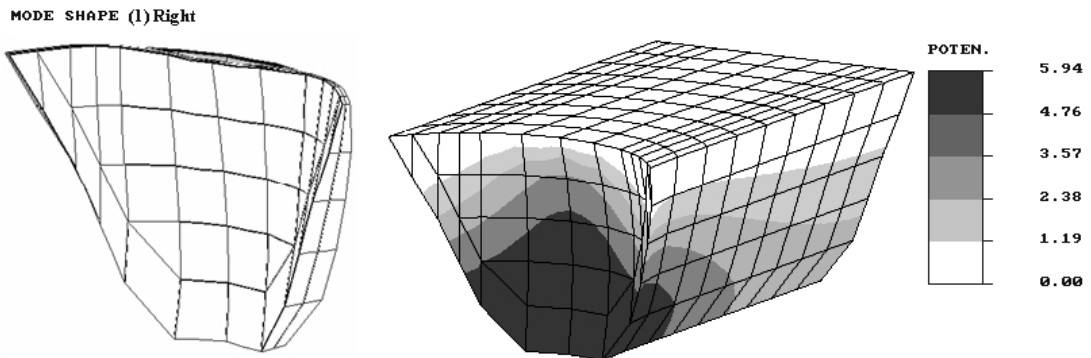


Figure 2. First right-mode shape of dam-reservoir system (Case M3)

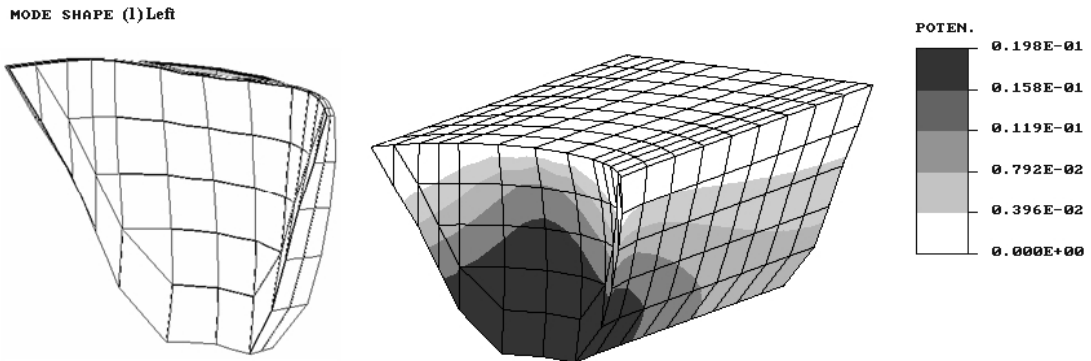


Figure 3. First left-mode shape of dam-reservoir system

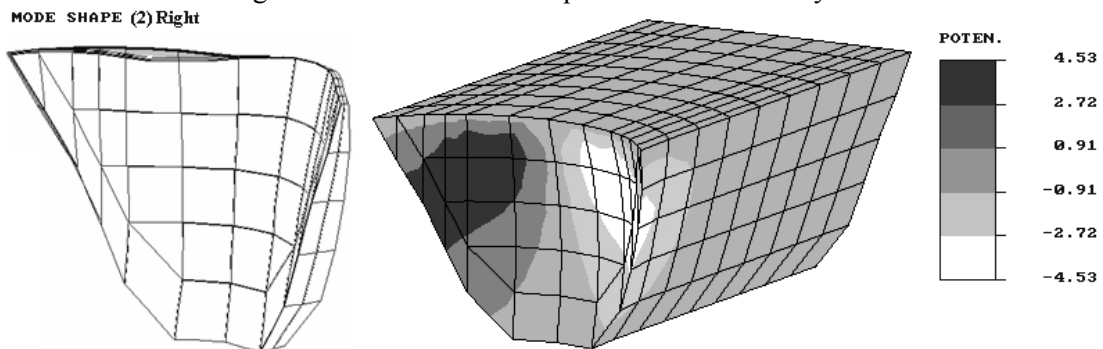


Figure 4. Second right-mode shape of dam-reservoir system

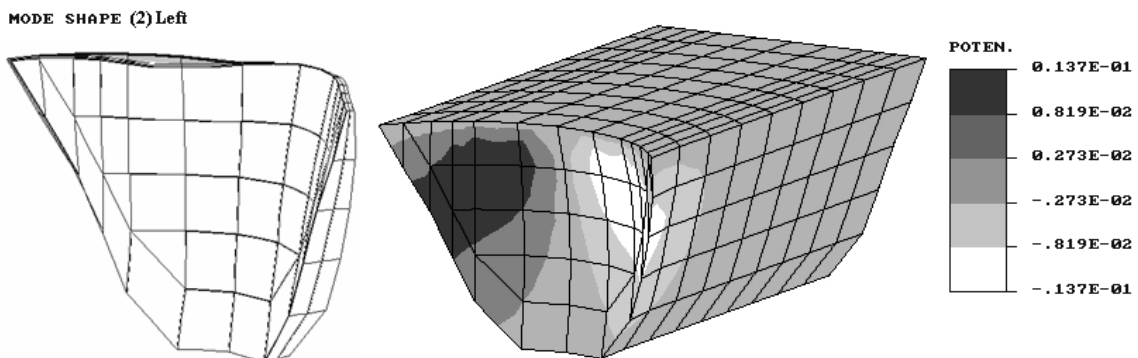


Figure 5. Second left-mode shape of dam-reservoir system

Execution time of mode shape computations for pseudo-symmetric subspace and modified unsymmetric Lanczos methods are presented in Tables 3 and 4, for comparison purposes.

Table 3.Computational time (sec.) for P.S.subspace

Case	No. of modes			
	5	10	20	50
M1	1.19	2.98	7.64	24.61
M2	2.70	8.50	52.08	170.09
M3	8.91	15.22	42.34	324.64
M4	21.02	38.36	81.49	283.45
M5	27.89	72.66	122.34	835.47
M6	42.86	94.59	197.50	1844.42

Table 4.Computational time (sec.) for M-Lanczos

Case	No. of modes			
	5	10	20	50
M1	1.89	4.55	10.93	43.16
M2	4.75	8.92	17.45	85.31
M3	5.61	14.83	31.77	145.63
M4	11.28	22.49	60.84	284.22
M5	17.80	35.06	111.83	430.30
M6	24.03	47.48	124.31	625.61

The results in these Tables indicate that execution times are relatively reduced for cases M3 to M6 regarding modified Lanczos method. This decline in execution time is accentuated especially for cases with higher degrees of freedom. Figure 6 provides a better illustration of computational time of modified Lanczos in comparison to Pseudo-symmetric subspace.

Figure 6a reveals that Pseudo-symmetric subspace is more efficient for cases with degrees of freedom up to 2400. This trend reverses with growth in number of degrees of freedom, and modified Lanczos method becomes much more efficient in comparison to Pseudo-symmetric subspace approach. It is also observed that for the case M6 (4210 DOFs), the modified Lanczos method leads to less execution time (i.e., 18.8 seconds) in comparison to Pseudo-symmetric subspace method. This is about 44% reduction of computational time. This trend is similarly extended to 10, 20 and 50 modes extraction for the case M6 where, 50%, 37% and 66% reduction in computational time has occurred.

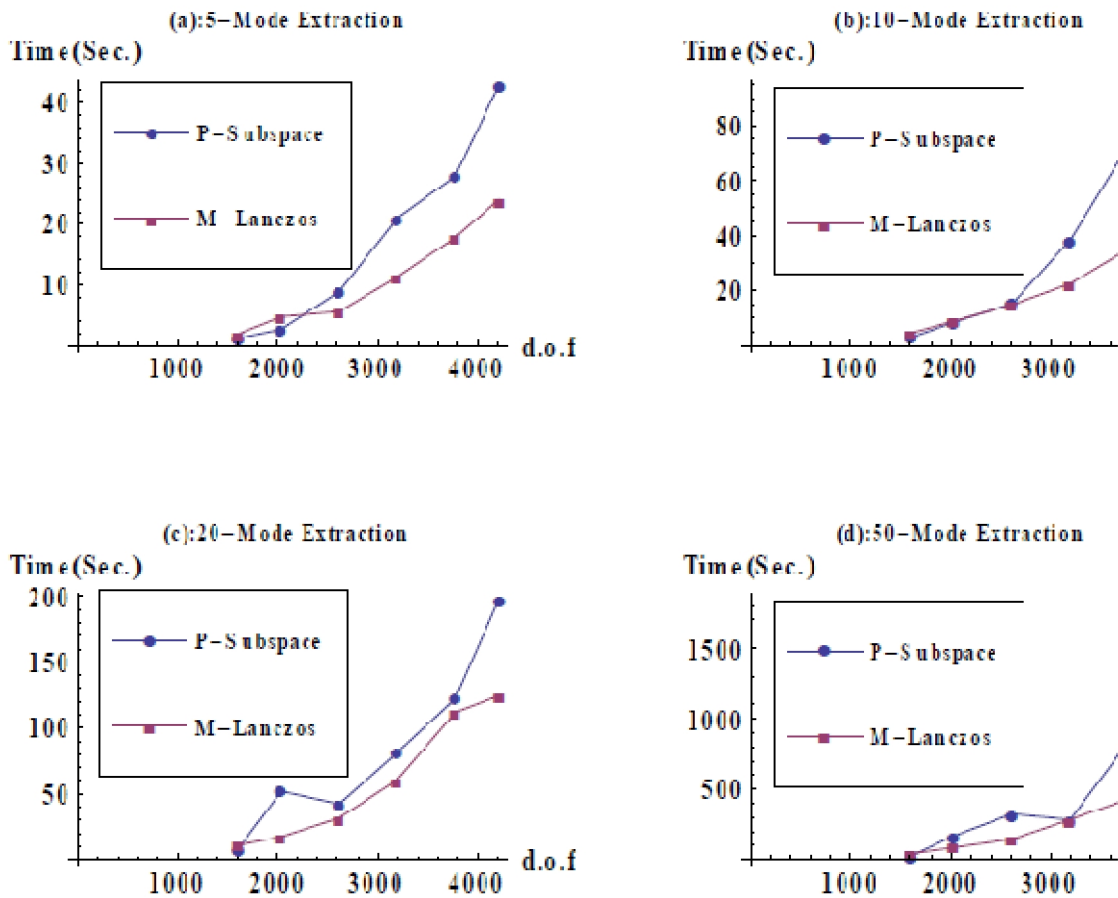


Figure 6. Computational time for pseudo-symmetric subspace and modified Lanczos methods

One of the main reasons for efficiency of the proposed method relates to number of participating vectors. In Pseudo-symmetric subspace approach, number of participating vectors for n -mode extraction is given by $m=\min(2n,n+8)$. While, spontaneous arithmetic operation is carried out on these vectors, modified Lanczos method starts with $2n$ sets of vectors where only two sets of vectors are used spontaneously in calculation. The latter method becomes much more efficient when degrees of freedom or number of modes are increased.

It is also worthwhile to mention that although, execution time reduction in mode extraction can be interpreted as an advantage for modified Lanczos over Pseudo-symmetric subspace, it should be noted that total number of implemented vectors in modified Lanczos exceed those of Pseudo-symmetric subspace and this requires extra memory allocation for that approach. Moreover, in general form of Lanczos, restarting in vectors might be required. However, no necessity for restarting was encountered in the present study for the modified version.

7. Conclusion

A proposed modified Lanczos method as well as Pseudo-symmetric subspace was presented in this paper. Developments in modified Lanczos method provided symmetric matrix implementation, skyline storage advantage and real-arithmetic considerations. Results indicated that modified Lanczos method demonstrates considerable time efficiency in contrast to Pseudo-symmetric subspace method. This is particularly true for cases with larger number of degrees of freedom. The least time reduction ratio for case M6 (4210 DOF) was 37% and this occurred when 20 mode were extracted. This ratio increased to 66% when 50 modes were requested.

References

- [1] J. Humar, M. Roufaiel, Finite element analysis of reservoir vibration. 1983;109(1):215-230.
- [2] Kl. Fok, AK. Chopra, Hydrodynamic and foundation flexibility effects in earthquake response of arch dams. ASCE, 1986.
- [3] A. Samii, V. Lotfi, Comparison of coupled and decoupled modal approaches in seismic analysis of concrete gravity dams in time domain. Finite elements in analysis and design. 2007;43(13):1003-1012.
- [4] B. Miquel, N. Bouaanani, Simplified evaluation of the vibration period and seismic response of gravity dam-water systems. Engineering Structures. 2010;32(8):2488-2502.
- [5] DW. Fausett, CT. Fulton, H. Hashish, Improved parallel QR method for large least squares problems involving Kronecker products. Journal of Computational and Applied Mathematics. 1997;78(1):63-78.
- [6] DS. Watkins, QR-like algorithms for eigenvalue problems. Journal of Computational and Applied Mathematics. 2000;123(1-2):67-83.
- [7] H. Zha, Z. Zhang, W. Ying, A quadratically convergent QR-like method without shifts for the Hermitian eigenvalue problem. Linear Algebra and its Applications. 2006;417(2-3):478-495.
- [8] G. Sandberg, A new strategy for solving fluid-structure problems. International Journal for Numerical Methods in Engineering. 1995;38(3):357-370.
- [9] G. Wu, An iterative block Arnoldi algorithm with modified approximate eigenvectors for large unsymmetric eigenvalue problems. Applied Mathematics and Computation. 2004;153(3):611-643.
- [10] M. Freitag, A. Spence, Convergence theory for inexact inverse iteration applied to the generalised nonsymmetric eigenproblem. Electronic Transactions on Numerical Analysis. 2007;28:40-67.
- [11] J. Berns-Müller, A. Spence, Inexact inverse iteration with variable shift for nonsymmetric generalized eigenvalue problems. SIAM J Matrix Anal Appl. 2006;28(4):1069-1082.
- [12] F. Xue, HC. Elman, Fast inexact subspace iteration for generalized eigenvalue problems with spectral transformation. Linear Algebra and its Applications. 2011;435(3):601-622.
- [13] Q. Ye, P. Zhang, Inexact inverse subspace iteration for generalized eigenvalue problems. Linear Algebra and its Applications. 2011;434(7):1697-1715.
- [14] C. Rajakumar, CR. Rogers, The Lanczos algorithm applied to unsymmetric generalized eigenvalue problem. International Journal for Numerical Methods in Engineering. 1991;32(5):1009-1026.

[15] K. Dookhitram, R. Boojhawon, M. Bhuruth, A new method for accelerating Arnoldi algorithms for large scale eigenproblems. *Mathematics and Computers in Simulation*. 2009;80(2):387-401.

[16] H-L. Liew, PM. Pinsky, Matrix-Padé via Lanczos solutions for vibrations of fluid–structure interaction. *International Journal for Numerical Methods in Engineering*. 2010;84(10):1183-1204.

[17] V. Lotfi, A. Aftabi Sani, Calculation of coupled modes of fluid-structure systems by pseudo symmetric subspace iteration methods. Submitted to the *Journal of Dam Engineering*. 2010.

[18] V. Lotfi, Seismic analysis of concrete dams using the pseudo-symmetric technique. *Journal of Dam Engineering*. 2002;XIII(2):119-145.

[19] BM. Irons, Role of part-inversion in fluid-structure problems with mixed variables. *AIAA Journal*. 1970;8(3):568-568.

[20] CA. Felippa, R. Ohayon, Mixed variational formulation of finite element analysis of acoustoelastic/slosh fluid-structure interaction. *Journal of Fluids and Structures*. 1990;4(1):35-57.

[21] JF. Hall, AK. Chopra, Dynamic analysis of arch dams including hydrodynamic effects. *Journal of Engineering Mechanics*. 1983;109(1):149-167.

Appendix

Table A1. Definition of special matrix operators

Matrix Presentation	Operator Function	Operator Notation
$\begin{bmatrix} \mathbf{A}_{11} & \mathbf{A}_{12} \\ \mathbf{A}_{21} & \mathbf{A}_{22} \end{bmatrix} \begin{matrix} 1 \\ * \end{matrix} \begin{bmatrix} \mathbf{X}_1 \\ \mathbf{X}_2 \end{bmatrix}$	$\begin{bmatrix} \mathbf{A}_{11} & \mathbf{A}_{12} \\ \mathbf{0} & \mathbf{A}_{22} \end{bmatrix} \begin{bmatrix} \mathbf{X}_1 \\ \mathbf{X}_2 \end{bmatrix}$	$\begin{matrix} 1 \\ * \end{matrix}$
$\begin{bmatrix} \mathbf{A}_{11} & \mathbf{A}_{12} \\ \mathbf{A}_{21} & \mathbf{A}_{22} \end{bmatrix} \begin{matrix} 2 \\ * \end{matrix} \begin{bmatrix} \mathbf{X}_1 \\ \mathbf{X}_2 \end{bmatrix}$	$\begin{bmatrix} \mathbf{A}_{11} & \mathbf{0} \\ \mathbf{A}_{21} & \mathbf{A}_{22} \end{bmatrix} \begin{bmatrix} \mathbf{X}_1 \\ \mathbf{X}_2 \end{bmatrix}$	$\begin{matrix} 2 \\ * \end{matrix}$
$\begin{bmatrix} \mathbf{A}_{11} & \mathbf{A}_{12} \\ \mathbf{A}_{21} & \mathbf{A}_{22} \end{bmatrix} \begin{matrix} 3 \\ * \end{matrix} \begin{bmatrix} \mathbf{X}_1 \\ \mathbf{X}_2 \end{bmatrix}$	$\begin{bmatrix} \mathbf{A}_{11} & \mathbf{0} \\ \mathbf{0} & \mathbf{0} \end{bmatrix} \begin{bmatrix} \mathbf{X}_1 \\ \mathbf{X}_2 \end{bmatrix}$	$\begin{matrix} 3 \\ * \end{matrix}$
$\begin{bmatrix} \mathbf{A}_{11} & \mathbf{A}_{12} \\ \mathbf{A}_{21} & \mathbf{A}_{22} \end{bmatrix} \begin{matrix} 4 \\ * \end{matrix} \begin{bmatrix} \mathbf{X}_1 \\ \mathbf{X}_2 \end{bmatrix}$	$\begin{bmatrix} \mathbf{0} & \mathbf{0} \\ \mathbf{0} & \mathbf{A}_{22} \end{bmatrix} \begin{bmatrix} \mathbf{X}_1 \\ \mathbf{X}_2 \end{bmatrix}$	$\begin{matrix} 4 \\ * \end{matrix}$
$\begin{bmatrix} \mathbf{A}_{11} & \mathbf{A}_{12} \\ \mathbf{A}_{21} & \mathbf{A}_{22} \end{bmatrix} \begin{matrix} 5 \\ * \end{matrix} \begin{bmatrix} \mathbf{X}_1 \\ \mathbf{X}_2 \end{bmatrix}$	$\begin{bmatrix} \mathbf{A}_{11} & \mathbf{A}_{12} \\ \mathbf{0} & \mathbf{0} \end{bmatrix} \begin{bmatrix} \mathbf{X}_1 \\ \mathbf{X}_2 \end{bmatrix}$	$\begin{matrix} 5 \\ * \end{matrix}$
$\begin{bmatrix} \mathbf{A}_{11} & \mathbf{A}_{12} \\ \mathbf{A}_{21} & \mathbf{A}_{22} \end{bmatrix} \begin{matrix} 6 \\ * \end{matrix} \begin{bmatrix} \mathbf{X}_1 \\ \mathbf{X}_2 \end{bmatrix}$	$\begin{bmatrix} \mathbf{0} & \mathbf{0} \\ \mathbf{A}_{21} & \mathbf{A}_{22} \end{bmatrix} \begin{bmatrix} \mathbf{X}_1 \\ \mathbf{X}_2 \end{bmatrix}$	$\begin{matrix} 6 \\ * \end{matrix}$

Note: Operator $\begin{matrix} 5 \\ * \end{matrix}$ is not used in this study.